# Selection of the Optimum *b* Factor for Diffusion-Weighted Magnetic Resonance Imaging Assessment of Ischemic Stroke

Peter B. Kingsley[1,2] and W. Gordon Monahan[1,2]

**The purpose of this study was to determine the diffusion sensitivity factor *b* that optimizes the contrast-to-noise ratio (CNR) for both diffusion-weighted signal intensity and the apparent diffusion coefficient (ADCNR) when evaluating ischemic stroke by diffusion-weighted MRI. The relative contrast, noise levels, CNR, and ADCNR were calculated for typical ADC values in human brain, 780 $\mu m^2/s$ in adults and 1200 $\mu m^2/s$ in neonates in normal tissue, 20–40% less in acute and subacute stroke, and 50% more in chronic stroke. The optimum *b* factor depends strongly on the ADC, whether TE is fixed or varies with the *b* factor, whether CNR or ADCNR is measured, and anisotropy. The optimum *b* factor in adults is 1000 s/mm$^2$ in acute and chronic stroke, and 1200 s/mm$^2$ in subacute stroke. The optimum values are about 200 s/mm$^2$ lower in neonates than in adults. The CNR and ADCNR are within 10% of the optimum over at least a 2-fold range of *b* factors, from 68–136% of the optimum *b* factor. If a single *b* factor is to be used for all situations, a diffusion *b* factor of 1000 s/mm$^2$ is recommended. Magn Reson Med 51:996–1001, 2004. © 2004 Wiley-Liss, Inc.**

**Key words: anisotropy; diffusion; infarct; optimization**

Diffusion-weighted magnetic resonance imaging (DWI) is widely used to assess acute, subacute, and chronic ischemic stroke (1–6). In acute stroke, tissue injury often is visible by DWI before changes are visible in conventional $T_1$-weighted or $T_2$-weighted images (3,4). Later, the apparent diffusion coefficient (ADC) can help to differentiate subacute infarction (less than 1 week old) from older chronic infarction and other conditions that are bright on $T_2$-weighted images (4–6).

In an anisotropic system like human brain, the measured ADC value, *D*, depends on the direction of the applied diffusion-sensitizing gradient, which can be applied in three orthogonal directions *x, y*, and *z*, separately or in combination. Typical white matter ADC values are 1200–1700 mm$^2$/s along the fibers and 200–400 mm$^2$/s perpendicular to the fibers (7). The amount of signal loss due to diffusion depends on the ADC and the diffusion sensitivity (*b* factor) according to:

$$S = P \exp(-TE/T_2)e^{-bD} = S_0 e^{-bD}, \quad [1]$$

where *P* is a function of the proton density and $S_0$ is the signal intensity without diffusion-sensitizing gradients ($b = 0$). Typically, a *b* factor of 1000 s/mm$^2$ has been used in stroke assessment due to hardware limitations (1). In anisotropic systems the average ADC, $D_{ave}$, is equal to the average of the ADCs measured in any three orthogonal directions, and this $D_{ave}$ results in a corresponding average DWI intensity $S_{ave}$. Therefore, DWI is usually performed three times, with the diffusion-sensitizing gradients in each of three orthogonal directions (such as *x, y, z*), so that:

$$D_{ave} = (D_x + D_y + D_z)/3 \quad [2]$$

$$S_{ave} = (S_x S_y S_z)^{1/3}. \quad [3]$$

Recently, it was suggested that a way to optimize the detection of acute infarcts was to maximize the signal intensity difference (contrast) between normal and infarcted tissues by using $b = 1500–2000$ s/mm$^2$ (1,2). The study by Pereira et al. (1) considered only isotropic diffusion with typical adult ADC values (an average of about 780 $\mu m^2/s$ in normal tissue and 463 $\mu m^2/s$, about 40% less, in ischemic tissue), identical signal intensity in normal and ischemic tissue when $b = 0$, and no change in TE when *b* changed. More important than simply the contrast is the contrast-to-noise ratio for signal intensities (CNR) and for ADC values (the apparent diffusion contrast-to-noise ratio, ADCNR). Although noise and CNR were mentioned previously, those articles only considered the noise in individual images, which is independent of the ADC and the *b* factor (1,2). Those articles did not consider how the noise in the original images affects the noise in the resulting average DW image (Eq. [3]) or ADC map when diffusion is anisotropic.

The purpose of the present work is to find the *b* factors that optimize CNR and ADCNR with anisotropic diffusion, with the increased ADC in neonatal brain, and with signal intensity changes caused by differences in $T_2$ or proton density. Calculations were performed both for the minimum TE at each *b* factor, $TE_{min}$, and for a fixed TE at all *b* factors.

## MATERIALS AND METHODS

### Effect of *b* Factor on Minimum TE

The minimum possible TE for an imaging sequence increases as *b* increases. Although it is impossible to determine a single precise relationship that is valid for all situations, the $TE_{min}$ for a given *b* value, or conversely the maximum *b* factor for a given TE, $b_{max}$, can be calculated for a standard pulse sequence (8). The formulas in (8)

[1]Department of Radiology, North Shore University Hospital, Manhasset, New York.

[2]Department of Radiology, New York University School of Medicine, New York, New York.

*Correspondence to: Peter B. Kingsley, Department of Radiology / MRI, North Shore University Hospital, 300 Community Drive, Manhasset, NY 11030. E-mail: pkingsle@nshs.edu

Received 2 September 2003; revised 25 November 2003; accepted 17 December 2003.

DOI 10.1002/mrm.20059
Published online in Wiley InterScience (www.interscience.wiley.com).

contain two errors: their eq. [15] should be $\Delta = TE/2 + t_B$ instead of $\Delta = TE/2 - t_B$, and in their eq. [16] -$\epsilon$ should be replaced by $+\epsilon$. The calculations presented here used a maximum gradient strength $G_{max}$ = 30 mT $m^{-1}$ unless otherwise specified, and $t_A$ and $t_B$ values similar to those of (8), $t_A = 34.86*22/G_{max}$ ms and $t_B$ = 4.4 ms.

For a given $G_{max}$, $TE_{min}$ can be decreased by using all three gradients instead of one gradient at a time. For example, using ($G_x$, $G_y$, $G_z$) = (1,-1,-1/2), (1/2,1,-1), and (1,1/2,1) provides three orthogonal gradient directions with the effective gradient strength increased by a factor $(1^2+1^2+0.5^2)^{0.5} = 1.5$ (9).

### Noise and Propagation of Errors

All calculations presented here assume that the SNR is high enough to assume Gaussian noise with no bias, and that the noise variance is $\sigma_0^2$. This assumption, which avoids the use of Rician statistics (10–13), is made explicitly or implicitly in the optimization of quantitative imaging (8,14). With this assumption, the noise in calculated images can be estimated from the noise in the original images by standard propagation-of-error formulas, which are of the form:

$$\sigma^2[f(x, y, z)] = \sigma_x^2\left(\frac{\partial f}{\partial x}\right)^2 + \sigma_y^2\left(\frac{\partial f}{\partial y}\right)^2 + \sigma_z^2\left(\frac{\partial f}{\partial z}\right)^2. \quad [4]$$

When the difference between two values is calculated, the variance of the difference is the sum of the individual variances, and the noise is the square root of the variance:

$$\text{Noise} = \sigma = (\sigma_i^2 + \sigma_n^2)^{1/2}. \quad [5]$$

Previous work has shown excellent agreement between propagation-of-error calculations and simulations (15), and between simulations and experimental data (15–17).

### Isotropic Diffusion

The contrast (signal intensity difference) between infarcted and normal tissue can be calculated by applying Eq. [1] to both infarcted and normal tissue:

$$\Delta S = S_i - S_n = S_{0i}\exp(-bfD_n) - S_{0n}\exp(-bD_n), \quad [6]$$

where $fD_n = D_i$ is the ADC in infarcted tissue. If TE is constant so that $S_{0n}$ and $S_{0i}$ do not change with $b$, then setting $d\Delta S/db = 0$ yields the $b$ factor for the maximum signal intensity difference $\Delta S_{max}$:

$$b_{\Delta S\,max} = \frac{\ln\left(\frac{D_n}{D_i}\right) - \ln\left(\frac{S_{0i}}{S_{0n}}\right)}{D_n - D_i}. \quad [7]$$

Equation [7] is equivalent to Eq. [3] in Ref. 1, except for the addition of the $\ln(S_{0i}/S_{0n})$ term. This equation, which is valid only if a fixed TE is used for all $b$ factors, provides an analytic solution for $b_{\Delta S max}$ (1).

### Anisotropic Diffusion

With anisotropic diffusion, no single $D$ value completely describes the system. In this case $D_n$ and $D_i$ are the $D_{ave}$ in normal and infarcted tissue, respectively (Eq. [2]). When three images are combined to produce a final image (Eq. [3]), the CNR and the optimum $b$ factor depend on how the noise in each initial image affects the final image. Previous work has generally assumed that the optimum $b$ factor for anisotropic diffusion was the same as for isotropic diffusion (8). The following calculations show that the optimum $b$ factor for anisotropic diffusion is always less than for isotropic diffusion.

With Gaussian noise the noise variance in the final DW image is found by applying Eq. [4] to Eq. [3], yielding:

$$\sigma^2(S_{ave}) = \sigma_0^2 S_{ave}^2[1/S_x^2 + 1/S_y^2 + 1/S_z^2]/9. \quad [8]$$

With isotropic diffusion $S_x = S_y = S_z = S_{ave}$ (Eq. [3]), so $\sigma^2(S_{ave}) = \sigma_0^2/3$.

Anisotropic diffusion is often modeled as cylindrically symmetric diffusion, with two of the three orthogonal axes of the diffusion ellipsoid being equal ($D2$) and the third direction possibly being different ($D1$), so that $D_{ave} = (D1 + 2*D2)/3$. This anisotropy is conveniently represented by the parameter $A$ of Ref. 18, which is identical to $A_{fiber} = -A_{disk}$ of Ref. 19 and can be expressed in terms of the ratio $D1/D2 = k$:

$$A = (D1/D_{ave} - 1)/2 = (k - 1)/(k + 2) \quad [9]$$

$$D1 = D_{ave}(2A + 1) \quad [10]$$

$$D2 = D_{ave}(1 - A), \quad [11]$$

where $A$ ranges from −0.5 for completely anisotropic oblate diffusion through 0 for isotropic diffusion to 1 for completely anisotropic prolate diffusion.

The individual signal intensities can be calculated from Eq. [1], contrast from Eq. [6], and the noise variance in the final diffusion-weighted signal intensity from Eq. [8]. After applying Eq. [8] to normal and ischemic tissues, substituting for $S_x$, $S_y$, and $S_z$ from Eq. [1] (using $D1$ and $D2$ from Eqs. [10] and [11]), and substituting for $S_i/S_{0i}$ and $S_n/S_{0n}$ from Eq. [1], the resulting CNR is:

$$CNR = \frac{3\Delta S}{\sigma_0\sqrt{e^{4AbD_i} + 2e^{-2AbD_i} + e^{4AbD_n} + 2e^{-2AbD_n}}}. \quad [12]$$

### Apparent Diffusion Contrast-to-Noise Ratios (ADCNR)

The numerator in the ADCNR is $D_n$-$D_i$, which is independent of image acquisition parameters, $T_2$ shine-through, or anisotropy. Calculation of the noise with Eqs. [4] and [5] is similar to previous similar derivations (14,20). The variance of $D_{ave}$ in a homogeneous tissue is:

$$\sigma_D^2 = \frac{9 + e^{2bD_x} + e^{2bD_y} + e^{2bD_z}}{9b^2SNR^2}. \quad [13]$$

Table 1
Parameters Used in the Calculation of Optimum *b* Factors

| Age and stage | *ADC* ($\mu m^2/s$) | $f(D_i/D_n)$ | $P_i/P_n$ | $T_2$ (ms) | Measure |
|---|---|---|---|---|---|
| Adults, normal | 780 | | 1 | 80 | |
| Acute | 468, 624 | 0.6, 0.8 | 1 | 80 | *CNR*[a] |
| Subacute | 468, 624 | 0.6, 0.8 | 1.2 | 104 | *ADCNR*[b] |
| Chronic | 1170 | 1.5 | 1.2 | 104 | *ADCNR* |
| Neonate, normal | 1200 | | 1 | 120 | |
| Acute | 720, 960 | 0.6, 0.8 | 1 | 120 | *CNR* |
| Subacute | 720, 960 | 0.6, 0.8 | 1.2 | 156 | *ADCNR* |
| Chronic | 1800 | 1.5 | 1.2 | 156 | *ADCNR* |

[a]*CNR*, contrast-to-noise ratio.
[b]*ADCNR*, apparent diffusion contrast-to-noise ratio.

After application of Eq. [13] to both infarcted and normal tissue, the resulting noise for the ADC difference between normal and ischemic tissue, $\sigma_{\Delta D}$, can be calculated as in Eq. [5], and the resulting ADCNR is:

$$ADCNR = (D_n - D_i)/\sigma_{\Delta D}. \quad [14]$$

### Choice of Numerical Values

The parameters used for calculations in acute, subacute, and chronic ischemia in adults and neonates are shown in Table 1. All calculations assume adult ADCs similar to those in Ref. 1, 780 $\mu m^2/s$ in normal brain tissue and 20% or 40% less in acute and subacute ischemia, with $T_2$ = 80 ms (8). In subacute ischemia $P_i$ is assumed to be 20% greater than $P_n$ ($P_i/P_n$ = 1.2), and $T_2$ is 30% greater (6). Calculations for chronic ischemia assume the same changes in $P_i/P_n$ and $T_2$, with a 50% ADC increase (3–5). In subacute and chronic ischemia, the optimum *b* factor with a fixed TE depends slightly on the value of the fixed TE, so $TE_{min}$ for the optimum *b* was used for all *b* factors.

Typical measurements in human brain yield ratios of $D_x$, $D_y$, and $D_z$ in the range $k$ = 1 to 4 (equivalent to $A$ = 0 to 0.5) (7), so calculations were performed with $A$ = 0.25 in adults. Reports of diffusion anisotropy in ischemic stroke suggest a steady decline in anisotropy over time (3,4,21,22), possibly with an initial increase (4,21). All calculations presented here assume no change in anisotropy in the ischemic region during acute and subacute ischemia, with a possible decrease during chronic ischemia.

In newborn infants the normal ADC is elevated, typically 1200 $\mu m^2/s$ (23–25), with less anisotropy ($k$ = 1 to 2, $A$ = 0 to 0.25) (24), and a $T_2$ about 50% longer than in adults (26,27)).

## RESULTS

### Effect of Changing TE When *b* Changes

Table 2 shows the $TE_{min}$ calculated for the commonly used value of $b$ = 1000 $s/mm^2$ at three different $G_{max}$, and when all three gradients are turned on at the same time in a 1:1:0.5 ratio. The optimum *b* factors for acute and subacute ischemia in adults with $f$ = 0.6 and $A$ = 0.25 are shown as a function of $G_{max}$ for $TE_{min}$ and with fixed TE.

The effects of changing TE when *b* changes were calculated for acute ischemia with isotropic diffusion, $f$ = 0.6, and $G_{max}$ = 30 mT/m in adults. The relative CNR and ADCNR as a function of *b* are shown in Fig. 1 for constant TE and for $TE_{min}$. For the constant TE, the $TE_{min}$ for the optimum *b* factor was used as the TE for all *b* factors, yielding TE = 102.6 ms for CNR and 104.7 ms for ADCNR. Thus, the two curves intersect at the optimum *b* factor for a constant TE. Compared to a fixed TE, with $TE_{min}$ the $b_{\Delta Smax}$ decreased 24% from 1637 to 1242 $s/mm^2$, and $b_{ADCNRmax}$ decreased 17% from 1806 to 1513 $s/mm^2$. These changes are consistent with previous observations (8).

### Acute Ischemia in Adults

In acute ischemia (about the first 12 hr) in adults, contrast is more important than ADC measurements because the

Table 2
Effect of Maximum Gradient Strength on $TE_{min}$ and Optimum *b* Factors

| $G_{max}$ (mT/m) | TE for $b$ = 1000 $s/mm^2$ | Acute | | Subacute | |
|---|---|---|---|---|---|
| | | $TE_{min}$ (ms) | $b_{CNRmax}$ ($s/mm^2$) | $TE_{min}$ (ms) | $b_{ADCNRmax}$ ($s/mm^2$) |
| 22 | 119.3 | 119.4 | 1005 | 122.6 | 1163 |
| 30 | 93.2 | 94.1 | 1053 | 96.6 | 1208 |
| 40 | 74.5 | 75.8 | 1092 | 77.8 | 1243 |
| 22 × 1.5[a] | 104.6 | 105.9 | 1083 | 107.9 | 1225 |
| 30 × 1.5[a] | 80.9 | 82.4 | 1118 | 84.0 | 1259 |
| 40 × 1.5[a] | 64.1 | 65.6 | 1146 | 67.0 | 1286 |
| | | Fixed[b] | 1307 | Fixed[b] | 1381 |

These calculations assume $f$ = 0.6 and $A$ = 0.25 in adults.
[a]Combining *x*, *y*, and *z* gradients to increase the effective diffusion $G_{max}$ by a factor of 1.5.
[b]Assuming that a fixed TE is used for all *b* factors.

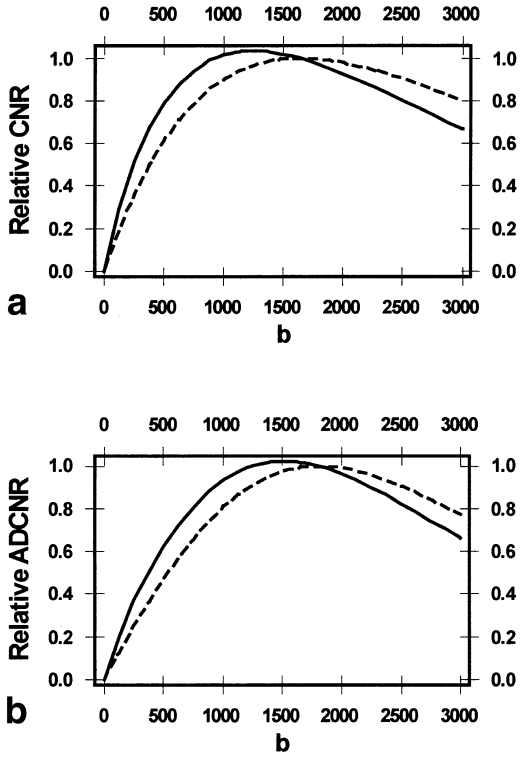


FIG. 1. Relative CNR and ADCNR as a function of *b* for acute stroke in adults with isotropic diffusion, $f = 0.6$, and $G_{max} = 30$ mT/m, with $TE_{min}$ (solid lines) and with constant TE (dashed lines). For the constant-TE calculations, TE was set equal to $TE_{min}$ for the optimum *b* factor.

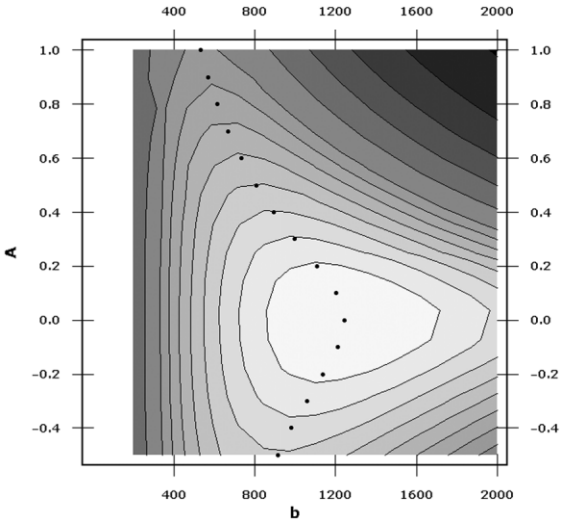


FIG. 2. Contour plot of relative CNR as a function of *b* and *A* for $f = 0.6$ in acute stroke in adults. CNR was calculated from Eqs. [6] and [12] with $TE_{min}$ and without $T_2$ changes ($S_{0i} = S_{0n}$). The dots show $b_{CNRmax}$ at several *A* values. *A* values less than zero correspond to oblate ellipsoids. Contours are at intervals of 5% of the maximum (which occurs at $A = 0$ and $b = 1242$ s/mm$^2$) from 95% to 60%, then at 10% intervals.

lesion is not even visible when $b = 0$. The optimum *b* factors are shown in Table 3. A contour plot of CNR as a function of *b* and *A* with $f = 0.6$ and $TE_{min}$ is shown in Fig. 2. For any given *b* value, CNR is maximum at $A = 0$ and decreases as anisotropy increases for both $A > 0$ and $A < 0$. As *A* increases in magnitude, $b_{CNRmax}$ decreases. Since $A = 0.25$ is an approximate average for human brain (7), the optimum *b* factor for DWI assessment of acute ischemic stroke in adults is about 1000 s/mm$^2$.

Because a range of effective *A* values is present in brain, the choice of an optimum *b* value should consider this range. The average CNR over the range $A = 0$ to $A = 0.5$ for $f = 0.6$ is maximum at $b = 1022$ s/mm$^2$, and the average value of $b_{CNRmax}$ over this range is 1047 s/mm$^2$. Both values are near $b_{CNRmax} = 1053$ s/mm$^2$ for $A = 0.25$, the middle of this range. This suggests that optimizing $bD_n$ at one *A* value provides nearly optimum results for a range centered at that *A* value.

### Subacute Ischemia in Adults

Within 12–24 hr, the $T_2$-weighted ($b = 0$) signal intensity in ischemic areas increases by about 50% above normal tissue, due to changes in $T_2$ and proton density (6). Contrast and CNR are maximum with *b* near or equal to 0

Table 3
Optimum *b* Factors (s/mm$^2$), and the *b* Factor Range Where *CNR* (Acute Stage) or *ADCNR* (Subacute and Chronic Stages) is Within 10% of the Maximum, for Different Ischemia Stages in Adults

| Stage | *f* | *A* | Optimum *b* | <10% Range | Optimum *b* with fixed TE |
|---|---|---|---|---|---|
| Acute | 0.6 | 0 | 1242 | 723–1979 | 1637 |
| (*CNR*) | 0.6 | 0.25 | **1053** | 634–1609 | 1307 |
| | 0.8 | 0 | 1104 | 646–1750 | 1430 |
| | 0.8 | 0.25 | **947** | 571–1445 | 1164 |
| Subacute | 0.6 | 0 | 1430 | 923–2058 | 1695 |
| (*ADCNR*) | 0.6 | 0.25 | **1208** | 802–1683 | 1381 |
| | 0.8 | 0 | 1403 | 901–2031 | 1666 |
| | 0.8 | 0.25 | **1187** | 783–1662 | 1359 |
| Chronic | 1.5 | 0 | 1122 | 728–1605 | 1291 |
| (*ADCNR*) | 1.5 | 0.25 | **937** | 626–1294 | 1044 |
| | 1.5 | 0.25, 0[a] | **1029** | 689–1496 | 1204 |

The most clinically important *b* factors are underlined and boldfaced.
[a]$A = 0.25$ in normal tissue, 0 in ischemic tissue.

Table 4
Optimum *b* Factors (s/mm$^2$), and the *b* Factor Range Where *CNR* (Acute Stage) or *ADCNR* (Subacute and Chronic Stages) is Within 10% of the Maximum, for Different Ischemia Stages in Neonates

| Stage | *f* | *A* | Optimum *b* | <10% Range | Optimum *b* with fixed TE |
|---|---|---|---|---|---|
| Acute | 0.6 | 0 | **911** | 540–1431 | 1064 |
| (*CNR*) | 0.6 | 0.25 | 754 | 463–1133 | 850 |
| | 0.8 | 0 | **804** | 479–1256 | 930 |
| | 0.8 | 0.25 | 675 | 415–1014 | 757 |
| Subacute | 0.6 | 0 | **1015** | 668–1444 | 1115 |
| (*ADCNR*) | 0.6 | 0.25 | 844 | 571–1161 | 908 |
| | 0.8 | 0 | **993** | 649–1421 | 1092 |
| | 0.8 | 0.25 | 826 | 556–1144 | 890 |
| Chronic | 1.5 | 0 | **763** | 504–1078 | 823 |
| (*ADCNR*) | 1.5 | 0.25 | 629 | 428–859 | 666 |

The most clinically important *b* factors are underlined and boldfaced.

s/mm$^2$, so it is important to optimize the higher *b* factor to measure ADC in order to distinguish subacute infarcts from older infarcts and other lesions. With $A = 0.25$, the optimum *b* factor for subacute ischemia in adults is about 1200 s/mm$^2$ (Table 3). A contour plot of ADCNR as a function of *b* and *A* with $f = 0.6$ and constant TE was similar to the CNR plot (Fig. 2), with slightly higher optimum *b* values and slightly steeper declines as one moved away from the optimum.

### Chronic Ischemia in Adults

The ADC gradually increases during subacute ischemia, eventually exceeding the ADC of normal tissue. These chronic infarcts may appear bright on DWI despite a high ADC, and anisotropy may decrease. ADC measurements can help to differentiate this $T_2$ shine-through from a recent (subacute) infarct. The optimum *b* factor for $A = 0.25$ is near 1000 s/mm$^2$ (Table 3).

### Ischemia in Neonates

In neonatal brain typical ADC values are 1200 μm$^2$/s compared to 700–800 μm$^2$/s in adult brain, with little or no anisotropy (23–25). The ADC increase causes optimum *b* factors to decrease considerably, while the decreased anisotropy causes a smaller increase in the optimum *b* factor (Table 4). In acute stroke, if one optimizes for a smaller ADC change of $f = 0.8$, or assumes a small amount of anisotropy (*A* between 0 and 0.25), the optimum *b* factor is about 800 s/mm$^2$, about 200 s/mm$^2$ less than in adults. The optimum *b* factors in subacute and chronic ischemia are also about 200 s/mm$^2$ less than in adults, or 1000 s/mm$^2$ in subacute ischemia and 800 s/mm$^2$ in chronic ischemia.

## DISCUSSION

When CNR and ADCNR were calculated for ischemic stroke in adults and neonates, the optimum *b* factor ranged from about 800 to 1200 s/mm$^2$ (Tables 3, 4). Results would be within 10% of the optimum for the most clinically relevant conditions (underlined boldface values in Tables 3, 4) with any *b* factor in the range 802–1078 s/mm$^2$. If a single *b* factor is used for assessment of ischemic stroke, it is better to keep the commonly used *b* factor of 1000 s/mm$^2$ rather than increase the *b* factor to 1500 s/mm$^2$ (1) or even greater (2). If a higher $G_{max}$ were available, such as in animal scanners or with gradient inserts in human scanners, the optimum *b* factors would increase slightly (Table 2). If the *b* factor can be optimized for each clinical case, the results may be improved slightly by increasing *b* to 1200 s/mm$^2$ in subacute ischemia in adults, and decreasing *b* to 800 s/mm$^2$ in acute and chronic ischemia in neonates.

Anisotropy has been considered previously in diffusion tensor imaging, and a method was suggested for ensuring that the precision of each of the six ADC measurements was above a selected minimum value over a specific ADC range (28). However, there do not appear to have been any publications concerning the optimum *b* factor for $D_{ave}$ calculations with anisotropy in DWI, as presented here.

Many factors contribute to the calculation of the optimum *b* factor, including age (adult or neonate), whether TE changes with *b*, whether one is measuring CNR or ADCNR, the amount of anisotropy, the amount of ADC change, $G_{max}$, and $T_2$ and proton density changes. The approximate relative importance of each factor can be seen by making individual changes from a reference condition of measuring CNR in acute ischemia in adults with $f = 0.6$, $A = 0.25$, $G_{max} = 30$ mT/m, and TE = $TE_{min}$ (Table 5). In addition, changes in $T_2$ and proton density strongly affect CNR and $b_{CNRmax}$, with much smaller effects on ADCNR and $b_{ADCNRmax}$. The importance of other factors compared to the ADC in determining the optimum *b* factor can be

Table 5
Changes From the Optimum *b* Factor of 1053 s/mm$^2$ by Changing One Parameter at a Time From a Reference Condition of Measuring *CNR* in Acute Ischemia in Adults With $f = 0.6$, $A = 0.25$, $G_{max} = 30$ mT/m, and TE = $TE_{min}$

| Parameter changed | Optimum *b* (s/mm$^2$) | % Change from reference |
|---|---|---|
| Age (neonate) | 754 | −28% |
| Fixed TE | 1307 | +24% |
| ADCNR | 1276 | +21% |
| $A = 0$ | 1242 | +18% |
| $f = 0.8$ | 947 | −10% |
| $G_{max} = 40$ mT/m, $x + y + z$[a] | 1146 | +9% |

[a]The *x*, *y*, and *z* gradients are applied together to increase the effective diffusion $G_{max}$ by a factor of 1.5 (see Table 2 and its accompanying text).

seen in Table 3 by comparing the optimum $b$ factor of 1053 s/mm$^2$ ($bD_i = 0.49$) in acute stroke with $D_i = 468$ mm$^2$/s ($f = 0.6$), $A = 0.25$, and variable TE, to the optimum $b$ factor of 1291 s/mm$^2$ ($bD_i = 1.51$) in chronic stroke with $D_i = 1170$ mm$^2$/s ($f = 1.5$), $A = 0$, and fixed TE.

The CNR and ADCNR were within 10% of the optimum values over a considerable range of $b$ factors, at least 62–150% of the optimum $b$ factor for CNR and 68–136% for ADCNR. Thus, nearly optimum results can be obtained over at least a 2-fold $b$ range for ADCNR and about a 2.5-fold $b$ range for CNR. Clearly, the exact choice of $b$ factor is not critical because a range of anisotropies, ADCs, and relative signal intensities will be present in both normal and ischemic tissue, and a considerable range of $b$ factors will yield results within 10% of the optimum (Tables 3, 4, Figs. 1 and 2) (14,28). However, it is still important to know approximate optimum $b$ factors in order to estimate the range of useful $b$ factors.

These results assume a monoexponential decay of signal intensity with increasing $b$ factor (Eq. [1]). Biexponential decay has been reported at high $b$ factors (9,29–31), and in infarcted tissue the relative fractions of the two components change slightly while their ADCs change much more (32). Although an exact calculation cannot be performed because of incomplete knowledge of the changes with ischemia, calculations with reasonable parameters (32) resulted in $b_{\Delta S\max}$ being changed by less than 1%. Calculations with other possible models resulted in $b_{\Delta S\max}$ decreasing by 19% or increasing by +6%. Thus, the presence of biexponential decay should have little or no effect on optimum $b$ factors.

## REFERENCES


1. Pereira RS, Harris AD, Sevick RJ, Frayne R. Effect of *b* value on contrast during diffusion-weighted magnetic resonance imaging assessment of acute ischemic stroke. J Magn Reson Imaging 2002;15:591–596.
2. Meyer JR, Gutierrez A, Mock B, Hebron D, Prager JM, Gorey MT, Homer D. High-b-value diffusion-weighted MR imaging of suspected brain infarction. AJNR Am J Neuroradiol 2000;21:1821–1829.
3. Zelaya F, Flood N, Chalk JB, Wang D, Doddrell DM, Strugnell W, Benson M, Ostergaard L, Semple J, Eagle S. An evaluation of the time dependence of the anisotropy of the water diffusion tensor in acute human ischemia. Magn Reson Imag 1999;17:331–348.
4. Yang Q, Tress BM, Barber PA, Desmond PM, Darby DG, Gerraty RP, Li T, Davis SM. Serial study of apparent diffusion coefficient and anisotropy in patients with acute stroke. Stroke 1999;30:2382–2390.
5. Beaulieu C, de Crespigny A, Tong DC, Moseley ME, Albers GW, Marks MP. Longitudinal magnetic resonance imaging study of perfusion and diffusion in stroke: evolution of lesion volume and correlation with clinical outcome. Ann Neurol 1999;46:568–578.
6. Burdette JH, Elster AD, Ricci PE. Acute cerebral infarction: quantification of spin-density and T2 shine-through phenomena on diffusion-weighted MR images. Radiology 1999;212:333–339.
7. Pierpaoli C, Jezzard P, Basser PJ, Barnett A, Di Chiro G. Diffusion tensor MR imaging of the human brain. Radiology 1996;201:637–648.
8. Jones DK, Horsfield MA, Simmons A. Optimal strategies for measuring diffusion in anisotropic systems by magnetic resonance imaging. Magn Reson Med 1999;42:515–525.
9. Mulkern RV, Vajapeyam S, Robertson RL, Caruso PA, Rivkin MJ, Maier SE. Biexponential apparent diffusion coefficient parametrization in adult vs newborn brain. Magn Reson Imag 2001;19:659–668.
10. Bernstein MA, Thomasson DM, Perman WH. Improved detectability in low signal-to-noise ratio magnetic resonance images by means of a phase-corrected real reconstruction. Med Phys 1989;16:813–817.
11. Gudbjartsson H, Patz S. The Rician distribution of noisy MRI data. Magn Reson Med 1995;34:910–914 [Erratum, related letter, and response: Magn Reson Med 1996;36:331–333].
12. Henkelman RM. Measurement of signal intensities in the presence of noise in MR images. Med Phys 1985;12:232–233 [Published correction: Med Phys 1986;13:544].
13. Edelstein WA, Bottomley PA, Pfeifer LM. A signal-to-noise calibration procedure for NMR imaging systems. Med Phys 1984;11:180–185.
14. Xing D, Papadakis NG, Huang CLH, Lee VM, Carpenter TA, Hall LD. Optimised diffusion-weighting for measurement of apparent diffusion coefficient (ADC) in human brain. Magn Reson Imag 1997;15:771–784.
15. Kingsley PB, Monahan WG. Effect of increased repetition time TR on precision of inversion-recovery $T_1$ measurements. Magn Reson Imag 2001;19:279–282.
16. Doran SJ, Attard JJ, Roberts TPL, Carpenter TA, Hall LD. Consideration of random errors in the quantitative imaging of NMR relaxation. J Magn Reson 1992;100:101–122.
17. Papadakis NG, Xing D, Huang CLH, Hall LD, Carpenter TA. A comparative study of acquisition schemes for diffusion tensor imaging using MRI. J Magn Reson 1999;137:67–82.
18. Conturo TE, McKinstry RC, Akbudak E, Robinson BH. Encoding of anisotropic diffusion with tetrahedral gradients: a general mathematical diffusion formalism and experimental results. Magn Reson Med 1996;35:399–412.
19. Ulug AM, van Zijl PCM. Orientation-independent diffusion imaging without tensor diagonalization: anisotropy definitions based on physical attributes of the diffusion ellipsoid. J Magn Reson Imag 1999;9:804–813.
20. Prasad PV, Nalcioglu O. A modified pulse sequence for in vivo diffusion imaging with reduced motion artifacts. Magn Reson Med 1991;18:116–131.
21. Green HAL, Peña A, Price CJ, Warburton EA, Pickard JD, Carpenter TA, Gillard JH. Increased anisotropy in acute stroke: a possible explanation. Stroke 2002;33:1517–1521.
22. Sorensen AG, Wu O, Copen WA, Davis TL, Gonzalez RG, Koroshetz WJ, Reese TG, Rosen BR, Wedeen VJ, Weisskoff RM. Human acute cerebral ischemia: detection of changes in water diffusion anisotropy by using MR imaging. Radiology 1999;212:785–792.
23. Lovblad KO, Ruoss K, Guzman R, Schroth G, Fusch C. Diffusion-weighted MRI of middle cerebral artery stroke in a newborn. Pediatr Radiol 2001;31:374–376.
24. Neil JJ, Shiran SI, McKinstry RC, Schefft GL, Snyder AZ, Almli CR, Akbudak E, Aronovitz JA, Miller JP, Lee BCP, Conturo TE. Normal brain in human newborns: apparent diffusion coefficient and diffusion anisotropy measured by using diffusion tensor MR imaging. Radiology 1998;209:57–66.
25. Robertson RL, Ben-Sira L, Barnes PD, Mulkern RV, Robson CD, Maier SE, Rivkin MJ, du Plessis AJ. MR line-scan diffusion-weighted imaging of term neonates with perinatal brain ischemia. AJNR Am J Neuroradiol 1999;20:1658–1670.
26. Holland BA, Haas DK, Norman D, Brant-Zawadzki M, Newton TH. MRI of normal brain maturation. AJNR Am J Neuroradiol 1986;7:201–208.
27. Masumura M. Proton relaxation time of immature brain. II. In vivo measurement of proton relaxation time ($T_1$ and $T_2$) in pediatric brain by MRI. Childs Nerv Syst 1987;3:6–11.
28. Armitage PA, Bastin ME. Utilizing the diffusion-to-noise ratio to optimize magnetic resonance diffusion tensor acquisition strategies for improving measurements of diffusion anisotropy. Magn Reson Med 2001;45:1056–1065.
29. Mulkern RV, Gudbjartsson H, Westin CF, Zengingonul HP, Gartner W, Guttmann CRG, Robertson RL, Kyriakos W, Schwartz R, Holtzman D, Jolesz FA, Maier SE. Multi-component apparent diffusion coefficients in human brain. NMR Biomed 1999;12:51–62.
30. Mulkern RV, Zengingonul HP, Robertson RL, Bogner P, Zou KH, Gudbjartsson H, Guttmann CRG, Holtzman D, Kyriakos W, Jolesz FA, Maier SE. Multi-component apparent diffusion coefficients in human brain: relationship to spin-lattice relaxation. Magn Reson Med 2000;44:292–300.
31. Clark CA, Le Bihan D. Water diffusion compartmentation and anisotropy at high *b* values in the human brain. Magn Reson Med 2000;44:852–859.
32. Niendorf T, Dijkhuizen RM, Norris DG, van Lookeren Campagne M, Nicolay K. Biexponential diffusion attenuation in various states of brain tissue: implications for diffusion-weighted imaging. Magn Reson Med 1996;36:847–857.